Minal and Prakash
Bioscience Nanotechnology (2025) 1:1
https://doi.org/10.1186/s44331-025-00001-7

Bioscience Nanotechnology

RESEARCH

Open Access

Green synthesis of Ag-Pd bimetallic nanoparticles and its efficacy against mosquito larvae and non-target organisms

Savy Panamkuttiyiel Minal[1*] and Soam Prakash[1]

Abstract

Background Emerging studies on bimetallic nanoparticles highlight their unique synergistic properties, but their efficacy and toxicity require further validation. Silver-palladium bimetallic nanoparticles (Ag-Pd BNPs), synthesized via eco-friendly biological methods, have demonstrated potential applications in catalysis, sensing, antimicrobial activities etc. However, data on their toxicity against invertebrates remains limited. The current study addresses this gap by presenting the eco-friendly synthesis of Ag-Pd BNPs using a nontoxic aqueous leaf extract of the plant *Citrus limon*. The synthesized nanoparticles were characterized using various techniques, and their efficacy was evaluated against mosquito larvae and nymphs of damselfly and dragonfly.

Results UV–Vis spectroscopy analysis showed maximum absorption at 300 nm ± 40 nm for the leaf extract, while for Ag-Pd BNPs an absence of a surface plasmon resonance band was observed. FT-IR spectroscopy analysis revealed the involvement of surface functional groups from the leaf extract in nanoparticle synthesis. TEM analysis determined a mean particle size of 21 ± 7 d nm. DLS analysis showed an overall hydrodynamic size of the nanoparticles clusters with a Z-average of 1956 d nm. SEM–EDX analysis verified the presence and purity of the Ag-Pd BNPs in the sample, and XRD results identified the leaf extract-mediated synthesis with distinct peaks obtained for Ag and Pd. The nano-toxicity efficacy of Ag-Pd BNPs revealed significant larval mortality against I, II, III, and IV instar larvae of both *Anopheles stephensi* and *Aedes aegypti* mosquito species, at 24 h, 48 h, and 72 h of exposure. The selected LC_{50} was further selected to study the predation efficiency of the non-target nymphs of damselfly and dragonfly which revealed time-dependent predation dynamics, resulting in high predation rates over specific time intervals.

Conclusion The present study offers significant scientific insights into an eco-friendly synthesis and characterization of Ag-Pd BNPs. Their inherent toxic ability to cause mortality in invertebrates like mosquito larvae underscores the need for caution in their environmental application. However, the absence of mortality among the odonate nymphs suggests the potential use of Ag-Pd BNPs in integrated vector management with optimized concentration. Future research can focus on developing controlled-release formulations to optimize environmental safety and facilitate easier remediation in natural ecosystems.

Keywords Bimetallic nanoparticles, Biological synthesis, Mosquito control, Nanotoxicity, Larvicidal efficacy

*Correspondence:
Savy Panamkuttiyiel Minal
savypanamkuttiyielminal@gmail.com
[1] Environmental Parasitology and Vector Control Nanobiotechnology Laboratory, Department of Zoology, Dayalbagh Educational Institute (Deemed University), Agra 282005, India

Background

Recent advancements in bottom-up approaches for metal nanoparticles (NPs) synthesis have increasingly focused on utilizing eco-friendly biological extracts. These extracts are derived from plants, microorganisms, and animal sources [1]. The metal nanoparticles

synthesized using biological extracts exhibit unique physicochemical properties, enabling their use in diverse applications [2]. These include efficient energy harvesting [3], photocatalytic materials [4, 5], strength enhancing anti-corrosive surface coatings [6, 7], development of new generation printing electronics [8], nanosensors [9, 10], toxicity evaluation [11], and extend to biomedical imaging and photo-thermal theragnostic applications [12–14]. Among various metal nanoparticles, silver (Ag) NPs have been extensively studied through biological synthesis methods and have demonstrated a wide range of bioactive properties, including antimicrobial [15, 16], antiparasitic [17], antifungal [18], and larvicidal activities [19, 20]. Additionally, they exhibit catalytic, imaging, therapeutic, and anticancer capabilities [21–23]. On the other hand, biologically synthesized palladium (Pd) NPs have gained significant attention due to their distinct physicochemical properties and size-dependent catalytic behaviour [24]. Furthermore, their bimetallic formulations have been recognized as unique materials because of the combined properties of the constituent metals. The incorporation of Pd in BNP formulations with other metals, such as silver or gold, often enhances the overall properties of biologically synthesized BNPs through combinatorial effects. This imparts BNPs with a distinct morphological composition and catalytic behaviour compared to their monometallic counterparts [25–27]. The biological synthesis of Ag-Pd BNPs has been investigated using various plant tissue extracts and resulting BNPs showed catalytic activities, such as Ag-Pd BNPs derived from the leaf extracts of, *Catharanthus roseus* demonstrated photocatalytic dye degradation activity against safranin O textile dye, *Cacumen platyclade* exhibited catalytic hydrogenation of 1,3-butadiene, while the leaf extract of *Lithodora hispidula* showed electrocatalytic reduction of hydrogen peroxide, and the gum kondagogu extract of *Cochlospermum gossypium* displayed catalytic potential in the degradation of 4-nitrophenol [28–31]. Moreover, the nut extract of *Prunus amygdalus*, as well as the fruit extracts of blackberry and *Terminalia chebula*, exhibited anticancer and antimicrobial activities [32, 33]. Lastly, Ag-Pd BNPs synthesized using a purified analytical grade biological pigment, rutin, have been successfully evaluated for its catalytic activity for the etherification reaction. The combined effects of Ag-Pd BNPs showed distinct properties compared to their monometallic forms, underscoring the need for further exploration of their activity in novel domains [34]. Considering the growing interest in the potential applications of Ag-Pd BNPs with antimicrobial activity, it is crucial to assess their ecotoxicity and potential use as an alternative to insecticides which is also a prerequisite to their environmental applications.

One of the most thoroughly investigated applications of nanoparticles lies in evaluating their larvicidal properties against ectoparasitic mosquitoes as the target organisms [35–41]. These mosquitoes, particularly adult females of the *Anopheles* species, play a pivotal role in transmitting various strains of the Plasmodium parasite, responsible for causing different types of malaria in humans and animals. In 2022, malaria accounted for 249 million positive cases and 608,000 deaths worldwide [42]. During the same period, there were documented cases and fatalities of diseases such as chikungunya, dengue, rift valley fever, yellow fever, and Zika virus fever, all transmitted by *Aedes* mosquito species, which act as vectors for these pathogens [43, 44]. A problem of climate change has led to the emergence of new breeding sites for adult mosquitoes in regions previously considered uninhabitable, as well as temporal shifts in breeding seasonality, have significantly influenced the dynamics of vector populations. Consequently, this raises substantial concerns regarding the potential burden of the emergence of vector-borne diseases in the future [45–48]. With the emergence of an insecticide-resistant population of mosquito species and the frequent occurrence of mosquito-borne diseases, it is crucial to search for alternative insecticidal tools for vector control, in addition to other integrated management approaches [49]. Moreover, ecotoxicological studies are now also focused on analyzing the effects of NPs against the non-target groups, including the natural enemies of mosquitoes such as nymphs of water bugs and odonates, crustaceans, and mosquito larvivorous fishes. This evolving field of study seeks to determine the minimal optimal concentration that ensures effectiveness without detriment to the natural biocontrol agents of mosquito vectors [50–52].

Phytochemical extracts obtained from various plant tissues and solvents have shown significant diversity in influencing the size and shape of synthesized nanoparticles [53, 54]. Furthermore, the toxic efficacy of nanoparticle formulations can vary depending on the intrinsic toxic properties of the biological extracts used in their synthesis [55]. Therefore, selecting a non-toxic reducing agent of biological origin is crucial in accurately assessing the toxicity of the synthesized nanoparticles. The aqueous leaf extract of plant like *Citrus limon* serves as an eco-friendly and biodegradable reducing agent, exhibiting non-toxic effects against mosquito larvae [56]. Consequently, its application facilitates precise and effective evaluation of the toxicity of the synthesized nanoparticles alone.

In the present study, we aimed to develop an eco-friendly and sustainable approach for synthesizing Ag-Pd

BNPs using a non-toxic and biodegradable aqueous leaf extract of plant *Citrus limon*. This approach aligns with the growing need for environmentally conscious methods in nanoparticles synthesis. The efficacy of synthesized Ag-Pd BNPs was evaluated against the larvae of two primary vectors of mosquito-borne diseases i.e., *Anopheles stephensi* and *Aedes aegypti*, across various instar stages (I, II, III, and IV) at 24 h, 48 h, and 72 h of exposure. Furthermore, recognizing the importance of minimizing unintended ecological impacts, we investigated the effect of the obtained LC_{50} concentrations on the predation efficiency of the dragonfly and damselfly nymphs. This evaluation aimed to identify potential non-target impacts of the selected LC_{50} obtained from the mosquito larvicidal bioassay, thereby contributing to their ecological safety profile.

Methods

All the methods were carried out in accordance with the Institutional guidelines and regulations.

Material

The study utilized analytical grade Silver nitrate (Merck Millipore), Palladium (II) chloride (HiMedia), hydrochloric acid (Merck), Whatman filter paper no.-1, and triple deionized (DI) water. For the larval bioassay, Temper (EC) (Temephos) insecticide was employed as the positive control. The biological specimens, including fresh leaves of *Citrus limon* (Linnaeus) Burm. f. (27°13′35.2"N 78°00′51.3"E), mosquito larvae of *Anopheles stephensi* (Liston) and *Aedes aegypti* (Linnaeus), as well as nymphs of Dragonfly (*Bradinopyga geminate)* and Damselfly (*Ischnura senegalensis*), were collected from the campus of Dayalbagh Educational Institute (DEI) in Agra, India (27°, 10′ N, 78° 05′ E).

Preparation of phytochemical extract

The bioactive constituents present in the leaves of the plant *Citrus limon*, were extracted using the hot-pot method [27]. In this method, 100 mg of minced leaves of plant *Citrus limon* were added to an Erlenmeyer flask containing 100 mL of DI water and heated at 65–70°C for 1 h on a hot plate. Subsequently, the plant debris was separated from the broth, and the resulting crude extract was filtered using Whatman filter paper no.-1 to obtain a purified 10% aqueous leaf extract, used for nanoparticles synthesis, stored at 4°C.

Synthesis of Ag-Pd BNPs

To synthesize Ag-Pd BNPs, 1 mM solutions of Silver nitrate ($AgNO_3$) and Palladium (II) chloride ($PdCl_2$ – HCl dissolved) were prepared in DI water and were separately mixed with the prepared 10% aqueous leaf extract of *Citrus limon*, in a ratio of 9:1. The mixtures were then kept in a dark environment for 1 h. Subsequently, the active solution of pre-Ag NPs was combined with the active solution of pre-Pd NPs in a 1:1 ratio. The resulting solution was a 2 mM pre-Ag-Pd BNPs solution, which was kept in the dark at room temperature overnight and then stored at 4°C.

Characterization

The prepared Ag-Pd BNPs (2 mM) and aqueous leaf extract (10%) samples were diluted in DI water in 1:10 and 1:9 ratios, respectively, and were characterized after 48 h of synthesis. Thereafter, the optical spectroscopy analysis with UV–Visible (UV VIS) spectrophotometer (Hitachi U-3900) and Fourier transform infrared (FT-IR) spectrophotometer (Bruker TENSOR 37 FTIR) for both leaf extract and Ag-Pd BNPs was performed. The micrographs of Ag-Pd BNPs (2 mM) were generated using Transmission Electron Microscopy (TEM) (Technai G 20 (FEI) TEM), and the sample was analyzed over formvar coated copper grids. The Ag-Pd BNPs sample was air-dried on the carbon tape substrate in a desiccator and was analyzed by Scanning Electron Microscope (SEM), the micrographs were obtained and the visualized area was further studied to determine the presence and composition of the Ag-Pd BNPs sample using Energy Dispersive X-ray (EDX) spectroscopy (SEM – Zeiss EV040 with PANalytical X'pert PRO). The hydrodynamic size of Ag-Pd BNPs was measured using Dynamic Light Scattering (DLS) analyzer (Malvern Zetasizer Ver. 7.12), and the crystalline nature of the nanoparticles was evaluated using X-ray Diffractometer (XRD) (D8 ADVANCE Bruker).

Preparation of mosquito larvae for bioassay

The collected larvae were initially separated into batches according to their developmental stages: II, III, and IV instar. To ensure accurate identification, online identification keys provided by the Walter Reed Biosystematics Unit (WRBU) were utilized [57]. The source water was further kept in a bio-incubator at 28 °C with a photoperiod of 8:16 h (L/D), to facilitate the hatching of newly emerged I instar larvae for both mosquito species. Prior to the bioassay, the mosquito larvae were washed twice with distilled water and morbid larvae were identified and removed from the batches to maintain a healthy and uniform larval population for the experiments.

Nanotoxicity bioassay

The evaluation of Ag-Pd BNPs in terms of nano-toxic efficacy was conducted following the guidelines outlined in the World Health Organization's manual on testing of mosquito larvicide (2005) [58]. The bioassay was

performed against I to IV instar larvae of both *Anopheles stephensi* and *Aedes aegypti* mosquito species. A wide range of test concentrations containing 25 larvae were assessed, and a specific range of concentrations was selected based on achieving 50% mortality after 24 h. The selected concentrations were 1.67, 3.34, 5, 6.67, and 13.34 mL/L of Ag-Pd BNPs were prepared in 150 mL of distilled water in a glass beaker. For each concentration, triplicates were prepared, each containing 25 larvae of same instars (either I, II, III, and IV) for both mosquito species, separately. For control groups, a positive control comprising 0.2% Temephos (EC) was used, along with two negative controls. One negative control consisted of 150 mL of distilled water, while the other negative control contained 13.34 mL/L of the prepared aqueous leaf extract (10%). The mortality rates within each test concentration and control groups were assessed at 24 h, 48 h, and 72 h or until 100% mortality was observed. The resulting data was analyzed to determine the effective lethal concentration (LC_{50}), which represents the concentration at which 50% mortality occurred in the test concentration.

Preparation of predatory nymphs

The collected nymphs of Dragonfly (*Bradinopyga geminata* (Rambur, 1842)) [59] and Damselfly (*Ischnura senegalensis* (Rambur, 1842)) [60] were identified using pictorial keys available in the Indian Biodiversity Portal. The identification process ensured accurate classification of the nymphs. Following identification, the nymphs of both species were individually placed in separate vessels. The vessels were provided with mosquito larvae, serving as a food source for the nymphs. This arrangement allowed the nymphs to acclimate and adapt to their environment, ensuring their readiness for the subsequent predator efficiency test.

Predation efficiency test

The rate of consumption of mosquito larvae by the predatory nymphs in the Ag-Pd BNPs test groups compared to the negative control groups was recorded to evaluate the predation efficiency. The nymphs of both dragonfly and damselfly measuring up to 1 inch in length, were selected as non-target test subjects. The LC_{50} value obtained from the larvicidal nanotoxicity bioassay against III instar larvae of both *Anopheles stephensi* and *Aedes aegypti*, at 24 h of exposure were selected for Ag-Pd BNPs test. Subsequently, four combinations (*Anopheles stephensi* with Dragonfly nymph, *Anopheles stephensi* with Damselfly nymph, *Aedes aegypti* with Dragonfly nymph, and *Aedes aegypti* with Damselfly nymph) were made by adding 25 III instar larvae and a nymph in a 250 mL glass beaker containing 150 mL of distilled water. The negative control contained only mosquito larvae and a nymph while the Ag-Pd BNPs test was obtained by adding the respective LC_{50} values to the prepared combinations. Each test and negative control (distilled water) were prepared in replicates (R1, R2, R3). The total predation process was observed at specific time intervals of 16 h, 20 h, 24 h, 40 h, 48 h, 64 h, and 72 h. The environmental conditions at the test site varied from 32–34 °C during the day and minimum to 24 °C during the night. To determine the % of predation efficiency achieved in each test and control groups, the formula: ((Number of consumed mosquito larvae / Number of predators) / Total number of mosquito larvae) × 100, was employed [61, 62].

Data analysis

The micropictographs obtained from TEM analysis were further analyzed using ImageJ software to generate a size distribution histogram of the nanoparticles, for the calculation of the mean particle size (in diameter nm) ± S.D. (standard deviation) [63]. The raw mortality data obtained from the nanotoxicity bioassay of Ag-Pd BNPs was subjected to Abbott's method (1925) [64] to determine the corrected mean mortality (%), i.e., when 5–20% mortality was observed in the negative control. This corrected mean mortality (%) values were then transformed into their respective probit values using the probit table (Finney 1948) [65]. Probit Analysis (Finney in 1952) [66] was used, the regression graphs were plotted for obtained probit values and the probit equations (ŷ-value) were generated to obtain LC_{50} values with its lower confidence limit (LCL) and upper confidence limit (UCL) at 95% Fiducial Confidence Interval (CI), through regression analysis using MS EXCEL. Additionally, LC_{50} ± S.D. (standard deviation) and S.E. (standard error), chi-squared (χ^2) test for the goodness of fit, and two-way ANOVA was also calculated. The transmittance peaks of FT-IR spectroscopy were analyzed as per the standard keys provided by Coates (2000) [67]. The graphs for characterization and probit analysis were plotted using the OriginPro 2023b [68].

Results

UV VIS spectroscopy analysis

The absorption spectra of the diluted samples (1:9) of aqueous leaf extract (10%) of plant *Citrus limon* (pH 5.29 at 29°C) exhibited the maximum absorbance in the UV region around 300 nm ± 40 nm (Fig. 1.A.a). Whereas, the diluted samples (1:10) of Ag-Pd BNPs (pH 1.26 at 29°C) showed absorption in the range of 380 – 500 nm without any distinct surface plasmon resonance (SPR) band (Fig. 1.A.b).

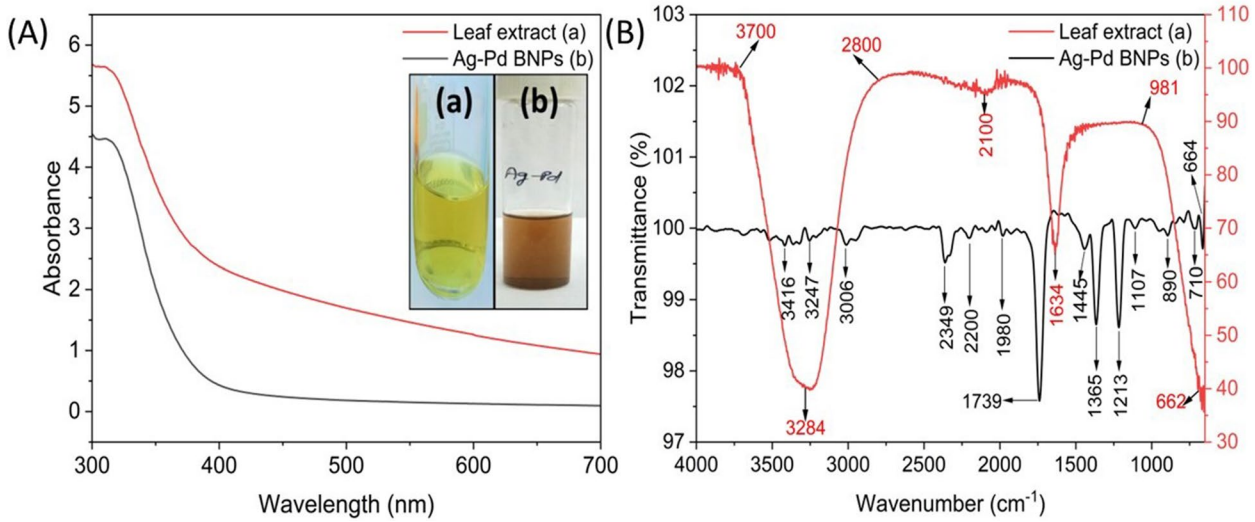

Fig. 1 **A** UV VIS absorption spectra; and (**B**) FT-IR transmittance spectra, for: (a) 10% aqueous leaf extract of plant *Citrus limon* (1:9) [inset A (a)], (b) diluted sample of Ag-Pd BNPs (1:10) [Inset A (b)

FT-IR spectroscopy analysis

Leaf Extract: The infrared spectrum of the aqueous leaf extract (Fig. 1.B.a) revealed a transmittance band with a broad peak (3700 cm^{-1}—~2800 cm^{-1}) corresponding to the stretching vibrations of the functional groups. These include O–H groups of intermolecular (high intensity peak) and intramolecular (weak intensity peak) bonded alcohols (3550–3200 cm^{-1}), N–H groups of amine salts (3000–2800 cm^{-1}), and overlapping C-H stretching vibrations of the alkane (3000–2840 cm^{-1}), alkene (3100–3000 cm^{-1}), and alkyne (3333–3267 cm^{-1}). A weak intensity peak around 2140–2100 cm^{-1} shows C≡C stretching of monosubstituted alkyne compounds, and C-H bending of aromatic compounds is present around 2000–1650 cm^{-1}. A medium-intensity peak showing C=C stretching of conjugated alkene (1650–1600 cm^{-1}), alkene di-substituted (cis) (1662–1626 cm^{-1}), cyclic alkene (1650–1566 cm^{-1}), and N–H bending was observed for amines (1650–1580 cm^{-1}). Another medium intensity peak for O–H bending of phenol compounds (1390–1310 cm^{-1}) is also observed and a characteristic strong intensity peak in the fingerprint region (1000–650 cm^{-1}) indicating the stretching and bending vibrations for C-H bending (900–700 cm^{-1}), C=C bending of alkene vinylidene compounds (895–885 cm^{-1}), and stretching vibrations of the halo compound groups such as C–Cl, C–Br, and C-I can be seen around 850–550 cm^{-1}, along with a peak for complex benzene derivatives around 700 $cm^{-1} \pm 20$ cm^{-1}. Ag-Pd BNPs: In contrast, the FT-IR spectra of Ag-Pd BNPs (Fig. 1.B.b) exhibited a highly reduced transmittance band between 3700 cm^{-1}—~2800 cm^{-1} compared to the leaf extract sample. The O=C=O stretching (2349 cm^{-1}) of carbon dioxide was observed, and a comparatively reduced fingerprint region (1000 cm^{-1} – 599 cm^{-1}) with weak intensity peaks can be seen in contrast to the strong intensity band of leaf extract. This change can be attributed to the utilization of the specific surface functional groups of leaf extract during nanoparticles synthesis.

TEM analysis

The micrographs of Ag-Pd BNPs samples (Fig. 2.A) revealed the presence of polydisperse electron-dense metal nanoparticles. These nanoparticles exhibited roughly irregular-spherical shape and displayed minimal agglomeration. The size distribution bins of the histogram (Fig. 2.B) generated for the TEM micrograph showed particles sizes ranging from 5 – 34 d nm (diameter in nm). The Gaussian fit analysis for the obtained particle size distribution bins showed a mean particle size (± SD) of 21 ± 7 d nm.

DLS analysis

The Zetasizer results (Fig. 3 A) for the diluted samples (1:10) of the Ag-Pd BNPs (2 mM) revealed a hydrodynamic size of the nano-clusters in the range of 800–1050 d nm. The Z-average was measured at 1956 d nm, with the peak (± S.D.) observed at 982 d nm (± 143 d nm), and a polydispersity index (PdI) of 0.5. This suggests that the sample has a larger hydrodynamic size of the nano-clusters compared to the actual size of the metal NPs within it as obtained from TEM analysis.

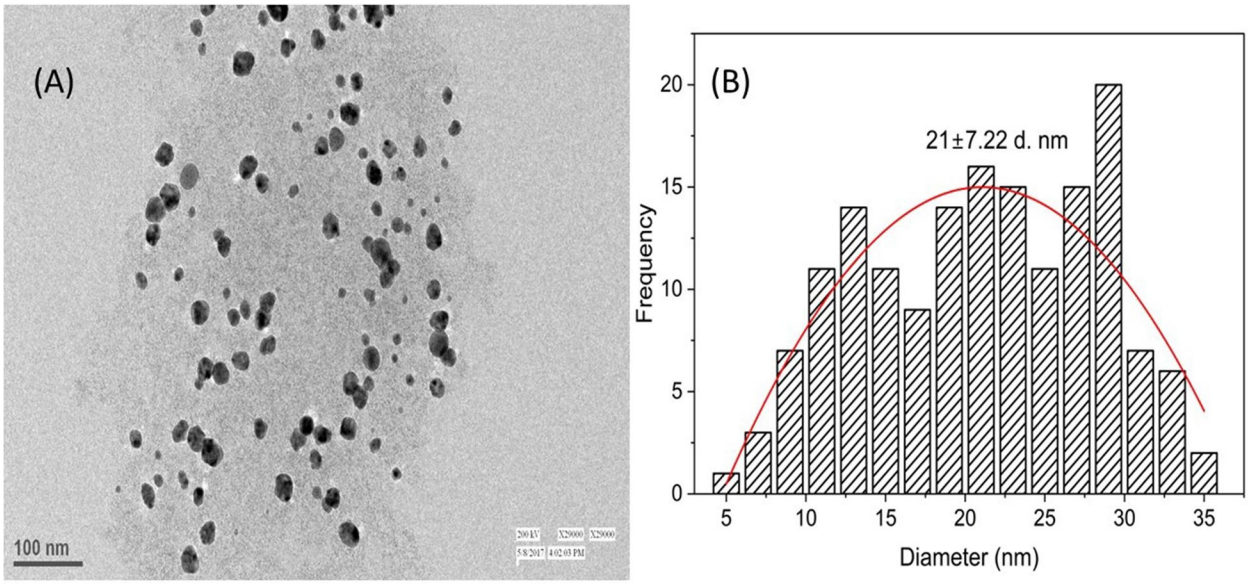

Fig. 2 **A** TEM micrograph of Ag-Pd BNPs (1:10), and (**B**) Particle size distribution histogram with Gaussian fit obtained from the ImageJ analysis of the TEM micrograph (**A**)

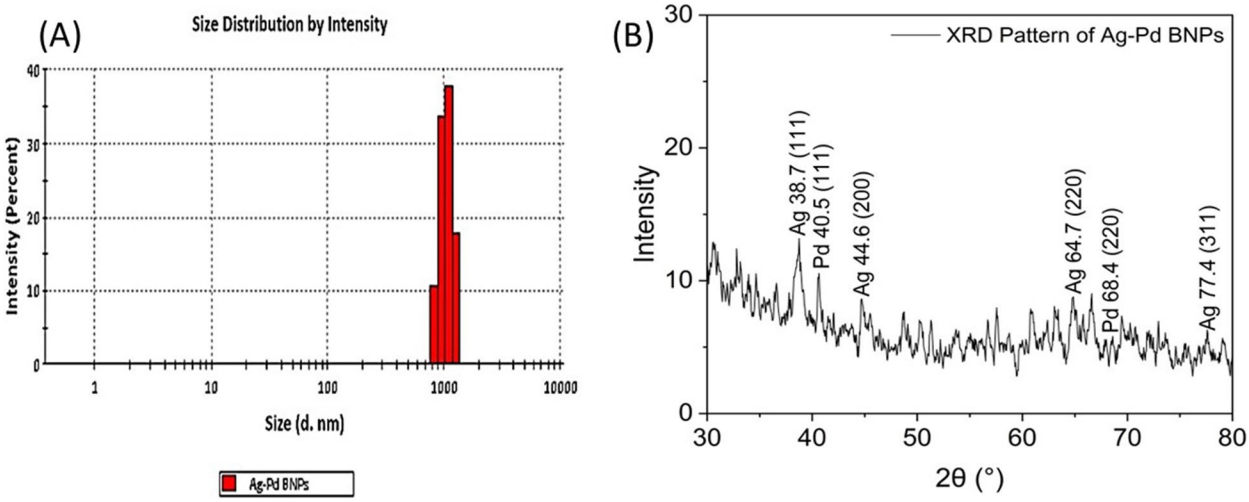

Fig. 3 **A** DLS of Ag-Pd BNPs (1:10), and (**B**) XRD pattern generated for Ag-Pd BNPs sample

XRD analysis

The results of XRD pattern for Ag-Pd BNPs samples (Fig. 3.B) revealed distinct peaks at 38.7°, 44.6°, 64.7°, and 77.4° corresponding to 2θ angle with lattice constants of (111), (200), (220) and (311), respectively. These peaks signify the presence of Ag particles in the sample, in accordance with the Ag content indicated by JCPDS no. 87–0720. Additionally, peaks at 40.5°, 48.6° and 68.4° of 2θ angle with lattice constants of (111), (200), and (220), respectively, were observed, indicating the presence of palladium in the sample as confirmed by JCPDS no. 65–6174. The high background noise and low-intensity peaks observed indicate the semi-crystalline nature of the Ag-Pd BNPs sample. This can be attributed to the synthesis process using leaf extract and low-concentration Ag-Pd BNPs present in the test sample.

SEM–EDX analysis

The illuminating surface containing Ag-Pd BNPs samples of SEM micrograph (Fig. 4.b) confirms the presence of metal nanoparticles. The peaks corresponding to Ag and Pd elements are present with an absence of the

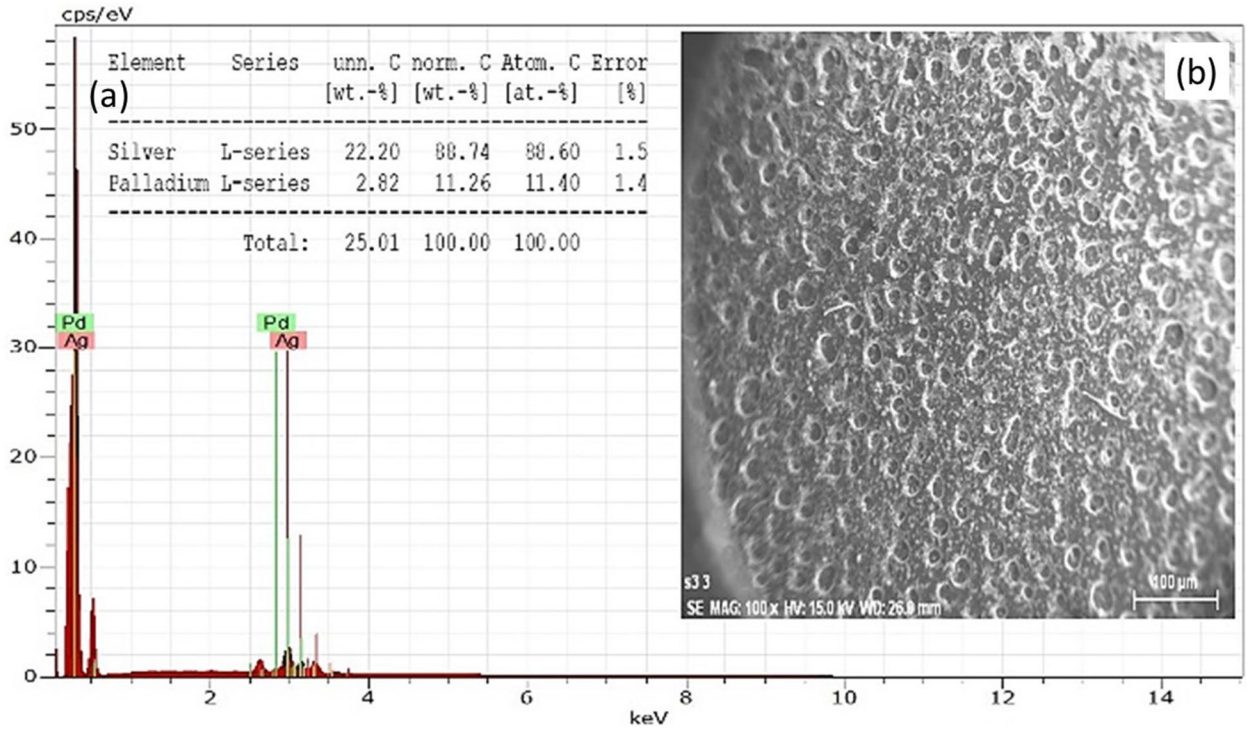

Fig. 4 SEM–EDX Analysis [inset: **a** EDX table for elements analysis result of the Ag-Pd BNPs samples shown in SEM micrograph (**b**)]

peaks related to other metal contaminants. The energy table (Fig. 4.a) generated from the EDX analysis of SEM micrograph shows the data generated from the L-series confirms the higher element % for silver (Ag) (88.74) as compared to palladium (Pd) (11.26), and with the atomic % of 88.60 for Ag and 11.40 for Pd, in the composites of Ag-Pd BNPs samples. This shows the content and composition of the formed nanoparticles (Ag-Pd BNPs), having a larger content of Ag as compared to Pd in the sample of formed Ag-Pd BNPs.

Nanotoxicity bioassay

The results of the Ag-Pd BNPs bioassay showed toxic efficacies against the I II, III, and IV instar larvae of selected mosquito species. The negative control containing distilled water and leaf extract showed no morbidity or mortality till 72 h of exposure. The positive control showed 100% mortality after 4 h. The mean corrected % mortality obtained [refer to Table 1 in supplementary material] from the bioassays was subjected to probit analysis and probit regression plots were generated for both *Anopheles stephensi* (Fig. 5.A) and *Aedes aegypti* (Fig. 5.B) for the calculation of the $LC_{50(LCL\text{-}UCL)}$ values with ± S.D. and S.E., against both mosquito species (Fig. 6.A.B) at 24 h, 48 h, and 72 h of exposure [refer to Table 2 and 3 in supplementary material].

Anopheles stephensi

For the Ag-Pd BNPs bioassay, the non-significant (NS) value of χ^2 test depicting the goodness of fit was obtained for the test concentrations against II, III, and IV instar larvae after 24 h of exposure. I instar: 100% mortality was observed at the lowest concentration of the Ag-Pd BNPs test concentration, and LC_{50} was estimated at around 0.10 mL/L. II instar: $LC_{50\ (LCL\text{-}UCL)}$ was observed at $1.59_{(1.08–2.33)}$ mL/L at 24 h. III instar: LC_{50} of $1.78_{(1.21–2.60)}$ mL/L at 24 h was observed. IV instar: LC_{50} of $1.62_{(1.12–2.34)}$ mL/L at 24 h was observed. The efficacy was observed till 72 h, however, the data analysis showed hypothetical LC_{50} values with a significant value of χ^2 test.

Aedes aegypti

The results obtained for Ag-Pd BNPs bioassay against *Aedes aegypti* showed the non-significant (NS) χ^2 test values depicting goodness of fit for the LC_{50} generated from the test concentrations against II (24 h), III, and IV instar larvae (24 h and 48 h). I instar: 100% mortality was observed with an LC_{50} value of 0.10 mL/L at 24 h of exposure. II instar: LC_{50} of $1.59_{(1.08–2.33)}$ mL/L at 24 h was observed. III instar: LC_{50} of $1.78_{(1.21–2.60)}$ mL/L at 24 h and $0.51_{(0.23–1.13)}$ mL/L at 48 h was observed. IV

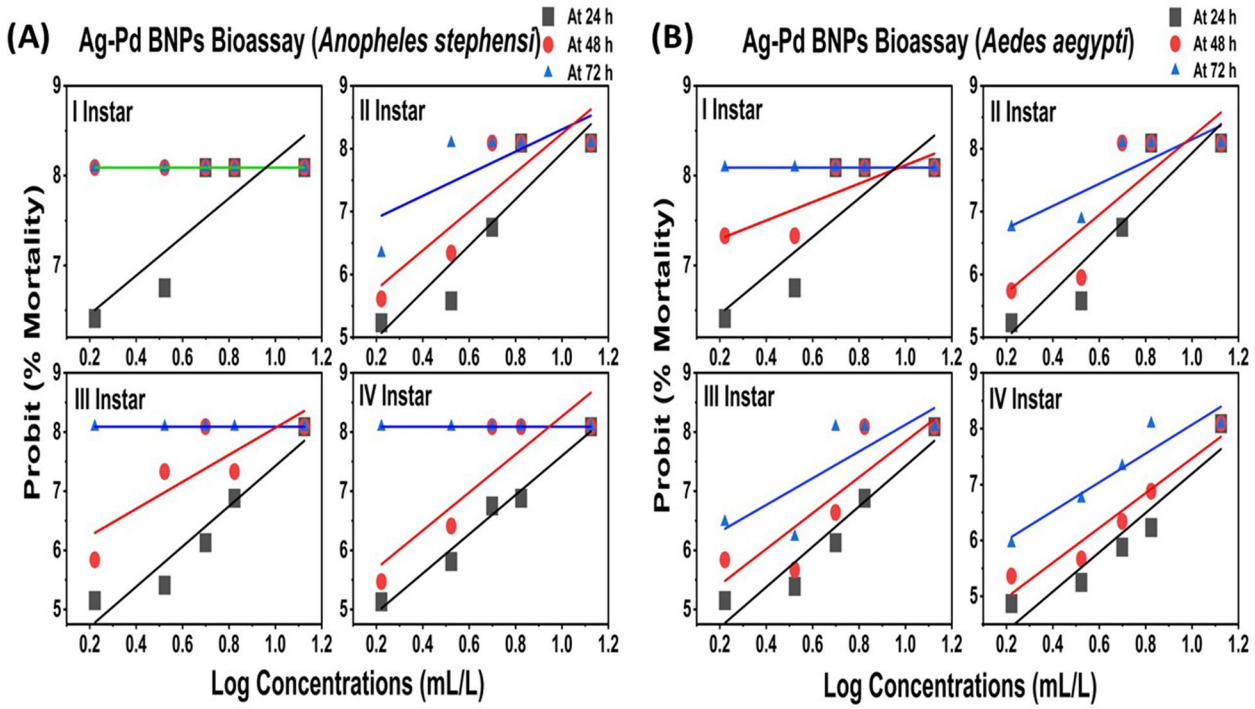

Fig. 5 Probit Analysis: Regression analysis to determine LC_{50} from the Ag-Pd BNPs bioassay against I-IV instar larvae of: **A** *Anopheles stephensi* (**B**) *Aedes aegypti*, at 24 h, 48 h, and 72 h of exposure

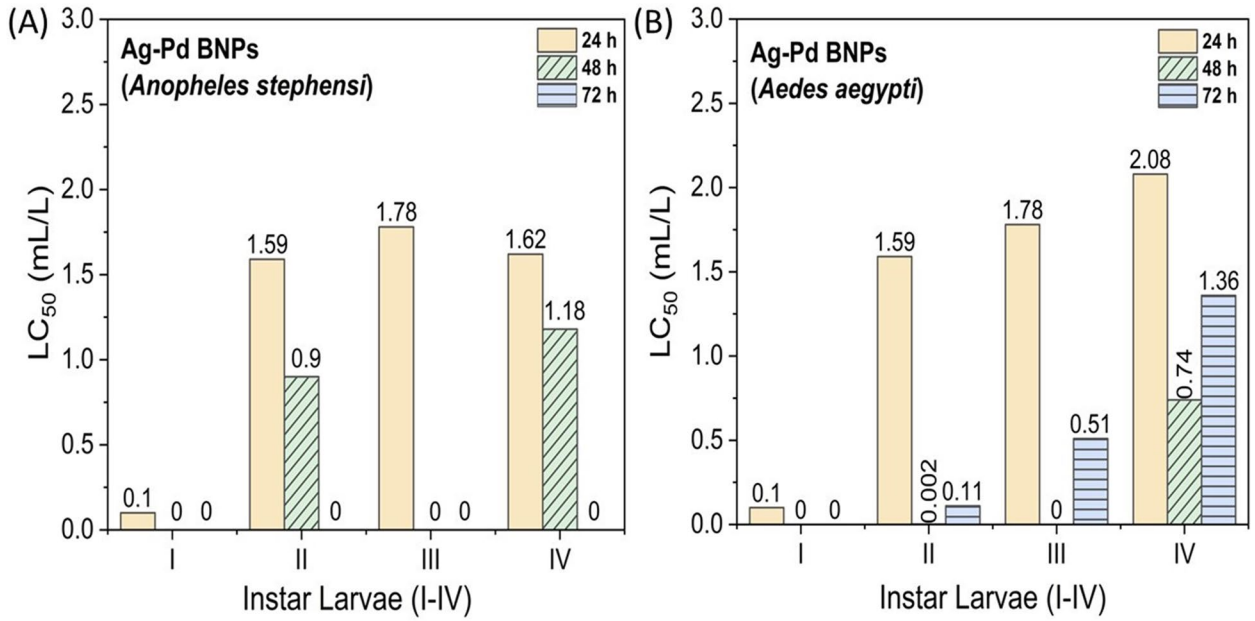

Fig. 6 Comparative LC_{50} value determined from the Ag-Pd BNPs bioassay against I-IV instar larvae of: **A** *Anopheles stephensi* (**B**) *Aedes aegypti*, at 24 h, 48 h, and 72 h of exposure

instar: LC_{50} of $2.08_{(1.37–3.16)}$ mL/L at 24 h and $1.36_{(0.87–2.14)}$ mL/L at 48 h was observed.

The results of two-way ANOVA showed a significant difference between the dependent variable i.e., obtained LC_{50} values after 24 h of exposure, against the independent variable i.e., mosquito species and larval Instar (II, III, and IV) [refer to Table 4.1 and 4.2 in supplementary material].

Predation efficiency test

The number of larvae consumed by each selected predatory nymph was recorded for the Ag-Pd BNPs test (LC_{50}) and negative control in replicates (R1, R2, R3) containing 25 III instar larvae of both mosquito species [refer to Table 5 and 6 in the supplementary material].

Negative control

The negative control groups, comprising of a dragonfly nymph with 25 III instar larvae of *Anopheles stephensi* exhibited 100% predation within 24 h (Fig. 7.A.a), and for *Aedes aegypti*, a complete predation was observed at 40 h (Fig. 7.A.b). Conversely, the negative control groups consisting of a damselfly nymph with 25 III instar larvae of *Anopheles stephensi* in each replicate, demonstrated 100% predation at 64 h (Fig. 7.A.c), whereas for *Aedes aegypti*, complete predation occurred at 40 h (Fig. 7.A.d).

Non-target organism bioassay

The LC_{50} value of 1.78 mL/L, obtained from the nano-toxicity bioassay using III instar larvae, was specifically selected as the benchmark for assessing the predation efficiency of the non-target organisms.

Dragonfly

LC_{50} (Anopheles stephensi): At 16 h, 55% of larvae were subject to predation, which increased to 71% at 20 h, 92% at 24 h, and ultimately reached 100% predation at 40 h (Fig. 7.B.a).

b. LC_{50} (Aedes aegypti): After 16 h, 61% of larvae were subjected to predation, rising to 73% at 20 h, 95% at 24 h, and achieving complete predation (100%) at 40 h (Fig. 7.B.b).

Damselfly

a. LC_{50} (Anopheles stephensi): At 16 h, predation resulted in the consumption of 51% of larvae, which increased to 84% at 20 h, 92% at 24 h, and ultimately achieved complete predation (100%) at 40 h (Fig. 7.B.c).

b. LC_{50} (Aedes aegypti): At 16 h, predation accounted for 76% of larvae, which further increased to 93% at 20 h, and eventually achieved complete predation (100%) at both 24 h and 40 h (Fig. 7.B.d).

The results obtained from the predation tests demonstrate a significant improvement in predation efficiency

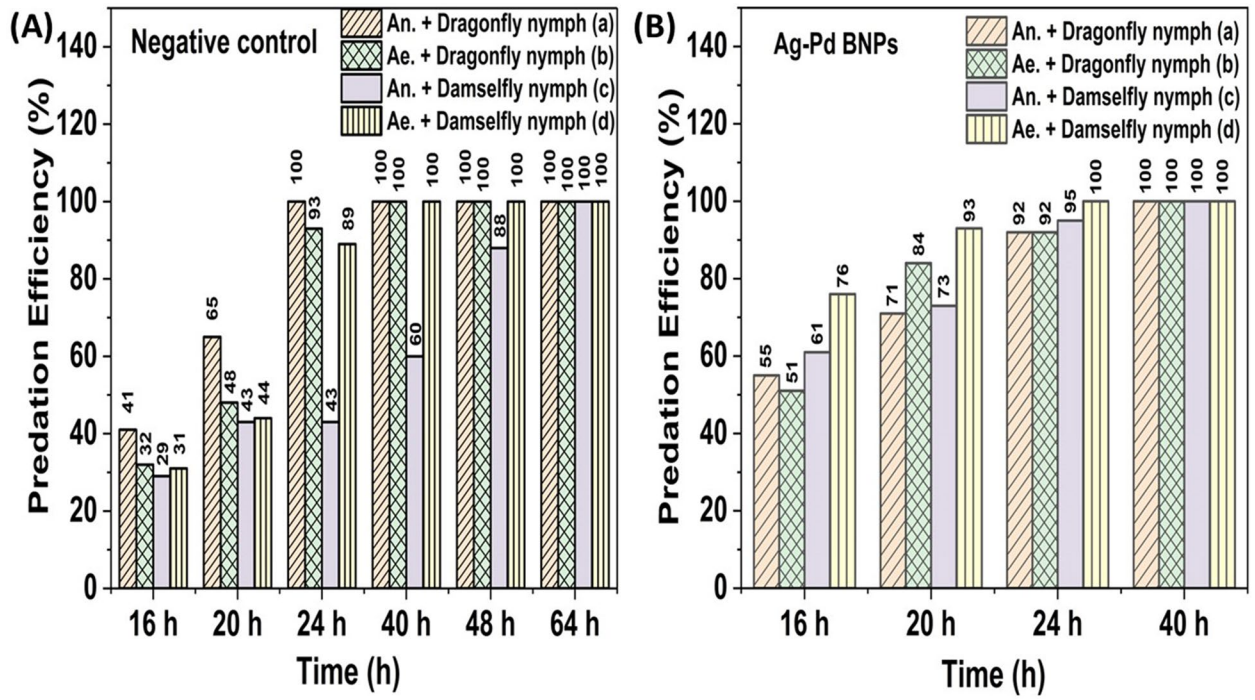

Fig. 7 Predation efficiency test of dragonfly (a, c) and damselfly (b, d) in (**A**) Negative Control, and (**B**) test concentration containing selected LC_{50} concentration of Ag-Pd BNPs, against the III instar larvae of both *Anopheles stephensi* (An.) *Aedes aegypti* (Ae.)

for the Ag-Pd BNPs test compared to the untreated control groups. The predatory nymphs exhibited resilience to the applied test concentration, as no mortality was recorded in any of the replicates during the 72 h observation period.

Discussion

UV VIS spectroscopy analysis

Generally, biologically synthesized Ag NPs exhibit a characteristic SPR band around 390–450 nm [19], while Pd NPs solution shows an absence of SPR band but the presence of absorption in the visible region, unlike the molar solution and leaf extract [40]. The absence of the SPR band in the current results aligns with the results of Ag-Pd BNPs synthesized using *Catharanthus roseus* leaf extract having an equal (1:1) Ag to Pd ratio by Mohan et al. (2021) [28]. This phenomenon of the absence of SPR band can be attributed to the combined effect of bimetallic properties resulting from the formation of Ag-Pd BNPs. Unlike silver, the specific electronic configuration of the palladium component of the Ag-Pd BNPs lacks the collective oscillation of loosely bound conduction band electrons which are responsible for the generation of the SPR band. Therefore, an absence of the SPR band depicts a shielding by the Pd component of BNPs which influences the SPR properties of Ag within the Ag-Pd BNPs BNPs. This was also observed for the Ag-Pd BNPs synthesized using fruit extract of *Terminalia chebula* by Sivamaruthi et al. (2019) [33]. Compared to our studies, Abdel-Fattah et al. (2017) [32], observed that the absence of the SPR band is linked with the Ag to Pd ratio. The use of relatively lower Ag concentrations, Pd:Ag (1:2), shows absence of an SPR band, consistent with our findings, which involved an equal concentration of both Ag and Pd (1:1). They further reported a prominent SPR band appeared in the formulation with higher Ag concentration (1:3, 1:4, 1:6 and 1:8), for the almond nut and blackberry fruit extract mediated Ag-Pd BNPs samples.

FT-IR spectroscopy analysis

These results are consistent with the reduced transmittance band of infrared spectra observed for the samples of *Cochlospermum gossypium* gum kondagogu extract mediated Ag-Pd BNPs (Velpula et al. (2021)) [31].

TEM analysis

The morphological variation in the size of biologically synthesized Ag-Pd BNPs using different extracts and methods is evident in the literature. Factors such as the type of extract used, Ag to Pd ratio, and duration of synthesis seem to play a role in determining the characteristic features of the synthesized BNPs and their properties for functions such as catalysis, antimicrobial activity, and anticancer effects, among others. The observed particle size in our study aligns with the findings of Sivamaruthi et al. (2019) [33], who successfully synthesized Ag-Pd BNPs (2–40 nm) with an average particle size of ~ 20 nm, using 1% *Terminalia chebula* fruit extract by reducing 10 mM $AgNO_3$ for 1 h, followed by the addition of 10 mM $PdCl_2$ in a 1:1 ratio. Similarly, Velpula et al. (2021) [31] reported comparable results using 1% gum kondagogu extract mediated Ag-Pd BNPs (2–40 nm) with a mean particle size of ~ 21 nm, obtained by reducing combined precursor solution of 1 mM $AgNO_3$ and $PdCl_2$ in 1:1 ratio. In another study, Mohan et al. (2021) [28] demonstrated the synthesis of Ag-Pd BNPs (1 mM, 1:1) using a 1% methanolic leaf extract of *Catharanthus roseus*, the resultant NPs exhibited a size distribution spanning 23–64 nm, with an average particle size falling within the range of 15–30 nm. In 2014, Lu et al. [29] reported the synthesis of monometallic nanoparticles mediated by *Cacumen platyclade* leaf extract. These nanoparticles exhibited an average particle size of 22 nm for Ag NPs and 7.3 nm for Pd BNPs. Additionally, the synthesis of bimetallic nanoparticles with various Ag to Pd ratios yielded particle sizes of 11.9 nm (3:1), 9.1 nm (1:1), and 7.4 nm (1:3) for Ag-Pd BNPs. Their findings indicated that a higher Pd concentration resulted in smaller particle sizes, which, in turn, demonstrated enhanced catalytic activity when compared to other nanoparticles.

DLS analysis

In comparison to our results, smaller hydrodynamic size of the biologically synthesized Ag-Pd BNPs was reported by Mohan et al. (2021) [28] in the range of 2–28 d nm with an average size of 28 d nm, while Velpula et al. (2021) [31] determined an average particle size of 44.8 d nm, and Sivamaruthi et al. (2019) [33] reported a range of 5–200 d nm with Z-average of 31.93 d nm. Turunc et al. (2017) [30] reported the average particle size of 15 d nm for Ag NPs and 22 d nm for Pd NPs, indicating a larger hydrodynamic size of smaller Pd NPs solution compared to Ag NPs. The DLS chart obtained by Abdel-Fattah et al. (2017) [32], showed the presence of Ag-Pd BNPs in the size range of 90–1200 d nm, which is close to our results. Yeap et al. (2018) [69] suggest that samples containing active interacting molecules tend to aggregate, resulting in larger-sized particles during DLS analysis compared to TEM analysis. According to Souza et al. (2016) [70] and Bhattacharjee (2016) [71], the aggregating properties of leaf extract biomolecules, which are used as capping and reducing agents, often contribute to NP retention and control their release in the environment.

XRD analysis

Similar to our results, the Ag-Pd BNPs synthesized using the leaf extract of *Cacumen platycladi* (Lu et al., (2014)) [29], gum kondagogu extract of *Cochlospermum gossypium* (Velpula et al. (2021)) [31, 34], and rutin biomolecule mediated synthesis showed identical X-ray diffractogram (Singh et al. (2020)) [34].

Nanotoxicity bioassay

Presently, the absence of comparative data for mosquito larvicidal bioassays involving Ag-Pd BNPs makes it challenging to establish a comparative relationship between particle size, toxicity (LC_{50}), and the type of extract used. However, our findings lay the groundwork for future comparisons of the efficacies of biologically synthesized Ag-Pd BNPs against larvae of mosquito vectors. Meanwhile, the monometallic NPs of Ag and Pd are well known to show toxic efficacies against mosquito larvae. One of the most effective formulations, containing an optimum concentration of Ag NPs, synthesized from the entomopathogenic fungus *Chrysosporium tropicum*, demonstrated larvicidal activity against *Culex quinquefasciatus* and *Anopheles stephensi*. The entomopathogenic nature of the fungus is advantageous for the biological management of insect pests. Furthermore, the addition of an optimal concentration of Ag NPs to the fungal broth has been shown to synergistically enhance the toxicity of the formulation, rather than inhibiting fungal growth. This enhancement extends the shelf life of the formulation thereby promoting its adhesion to the insect cuticle, leading to fungal infestation in the insect pest. Such strategic formulations contribute to reducing environmental implications by decreasing reliance on chemical insecticides and enhancing the effectiveness of biological control methods (Soni and Prakash (2012)) [72]. Bhakyara et al. (2017) [73], observed that the Pd NPs synthesized using a toxic leaf extract of plant *Melia azedarach*, showed greater larvicidal toxicity against III instars of *Aedes aegypti* with LC_{50} obtained at 27.36% as compared to the leaf extract alone with LC_{50} at 93.96% at 24 h. Therefore, the combined toxic effect with the leaf extract can contribute to the overall toxicity which can be further enhanced by the additional synthesized Pd NPs in an optimum concentration. Conversely, Minal and Prakash (2018) [40], used a non-toxic leaf extract of *Citrus limon* for Pd NPs synthesis and reported an LC_{50} value of 16.038% at 24 h of exposure against III instar larvae of *Anopheles stephensi*, thus emphasizing the intrinsic toxic efficacy of Pd NPs without a significant contribution from the leaf extract. An attempt to elucidate the mechanism of action leading to larval mortality induced by these nanoparticles was conducted by Kalimuthu et al. (2017) [74] through histological studies of *Hedychium coronarium* rhizome-mediated Ag NPs treated IV instar larvae of *Aedes aegypti*. Their findings indicated that, in comparison to the untreated control group, the mid-gut of the treated larvae exhibited partial lysis of the epithelium at the apical side. This was attributed to swollen epithelial cells filled with multiple vacuoles, and the lumen contained the content of ruptured epithelial cells. The physiological damages caused by Ag NPs were further analyzed at the cellular and biochemical levels by Fouad et al. (2017) [75], using *Cassia fistula* fruit pulp extract-mediated Ag NPs against the IV instar larvae of *Aedes albopictus* and *Culex pipiens pallens*. They reported a considerable decrease in the total protein content and downregulation of two key enzymes, namely Acetylcholinesterase and α- and β-carboxylesterase. In addition to these three biochemical parameters, Ga'al et al. (2017) [76] also reported the downregulation of acid and alkaline phosphatase due to Ag NPs synthesized with the green method using salicylic acid and its derivative, 3,5-dinitrosalicylic acid. These changes demonstrate the direct toxic effect of the Ag NPs, resulting in abnormal physiology, and cell signalling alterations, often leading to cell lysis, and a reduction in metabolic and neuromuscular activity. Moreover, the inability of downregulated and damaged α- and β-carboxylesterase enzymes to further detoxify the cell leads to the accumulation and aggregation of the metal NPs in the system, which is the main cause of larval mortality in the nanotoxicity bioassay. Thereby, making NPs the most suitable alternative against mosquito species resistant to chemical and biological insecticides, while simultaneously raising concerns about its effects on other non-target environmental organisms.

Predation efficiency test

The increased predation rates, however, may be a response to meet the energy demand for defense against the metal stress induced by the Ag-Pd BNPs test in the nymphs. dos Santos Lima et al. (2021) [77] investigated disruptions in the food web caused by metal stress from copper, cadmium, mercury, and manganese. The study aimed to examine how this metal stress influenced biotic interactions, specifically focusing on the feeding preferences and predation rates of dragonfly nymphs (*Tramea cophisa*) and ostracods (*Chlamydotheca* sp.) on water-dwelling crustaceans. The research revealed that, although metal stress did not alter food preferences, it did modify predation behaviour in a species-specific and metal-specific manner. Overall, a decrease in predation rates was observed for dragonfly nymphs, while increased predation rates were noted for ostracods. Hence, this study establishes that the enhanced predation rate of nymphs induced by nanoparticles may not necessarily be beneficial for the well-being of the predatory nymph.

Azam et al. (2015) [78] found the libellulid dragonfly (*Crocothemis servilia*) to be a highly effective ecological indicator for water and riparian systems. They observed that heavy metal-induced stress not only alters the life history of insects but also makes them efficient bio-indicators due to metal bioaccumulation, offering a clear measure of heavy metal contamination across different locations. Similarly, a study conducted by Akhtar et al. (2021) [79] demonstrated the occurrence of bio-transfer and bioaccumulation of various heavy metals between the trophic levels of the food chain from mosquito larvae to natural predators, such as dragonfly nymphs (*Tramea cophysa*), frequently resulting in the mortality of nymphs due to higher metal bioaccumulation. A notable decrease in the mobility of mosquito larvae from both species under the applied nanotoxicity bioassay can be a factor influencing predation efficiency, contributing to the accelerated predation by nymphs within the experimental setup. Likewise, in a study conducted by Murugan et al. (2015) [80], it was demonstrated that the specified lower concentration of synthesized Ag NPs could effectively induce mortality in *Anopheles* larvae, while it had no apparent impact on the predation efficiency of dragonfly nymphs (*Anax immaculifrons*). Studies conducted on natural copepod predators (*Mesocyclops longisetus, Mesocyclops aspericornis*, and *Megacyclops formosanus*) which are found to be effective against the I and II instars of *Anopheles* and *Aedes* mosquito species, revealed an increase in predation at lower test concentrations of Ag NPs without resulting in predator mortality. Conversely, higher concentrations of Ag NPs led to predator mortality, suggesting the need for lower doses to ensure that natural copepod predators are not adversely affected by Ag NPs (Murugan et al. (2015) [81], Murugan et al. (2016b) [82], Kalimuthu et al. (2017)) [83]. Therefore, the observed increase in predation rates in our study compared to the control group may be attributed to metal stress. While the selected concentration of Ag-Pd BNPs has not adversely affected the nymphs directly, their feeding on the Ag-Pd BNPs-affected, slowed larvae could lead to further bioaccumulation of nanoparticles from prey to predator through the food chain. This process may eventually result in complications and the ultimate death of the natural biocontrol agents. Consequently, we recommend future studies on a comparatively long-term investigation of the effects of nanoparticle bioaccumulation on the normal continuity of the life cycle of non-target organisms.

Despite the absence of studies on biologically synthesized Ag-Pd BNPs against both target mosquito larvae and non-target predatory organisms, there are existing studies on the antimicrobial and anticancer activities of Ag-Pd BNPs. Abdel-Fattah et al. (2017) [32] synthesized Ag-Pd BNPs using almond nuts and blackberry fruit extracts separately, incorporating varying Pd (1) to Ag (2,4,6, and 8) ratios-specifically, 1:2, 1:3, 1:4, 1:6 and 1:8. The almond nuts extract-mediated Pd–Ag BNPs (1:6) and blackberry fruit extract-mediated Pd–Ag BNPs (1:8) were selected for TEM analysis, showing the formation of 8 nm and 6 nm nanoparticles, respectively. These Ag-Pd BNPs, mediated from both extracts, demonstrated cytotoxicity against human breast cancer (MCF7) and liver cancer (HEPG2). Notably, a Pd:Ag ratio of 1:3 exhibited maximum mortality at the half-maximal inhibitory concentration (IC_{50}), outperforming Ag-Pd BNPs with a Pd:Ag ratio of 1:8. This highlights the significant impact of the Pd to Ag ratios used in the formulation. Additionally, in the antimicrobial assay against bacterial strains such as *Escherichia coli* and *Staphylococcus aureus*, as well as fungal strain of *Candida albicans*, Ag-Pd BNPs with a Pd:Ag ratio of 1:8 outperformed those with lower Ag ratios, shedding light on the cell-specific and composition-specific activity of Ag-Pd BNPs. Sivamaruthi et al. (2019) [33] observed that Ag-Pd BNPs mediated by *Terminalia chebula* fruit extract exhibited substantial antimicrobial activity against bacteria, including methicillin-resistant *Staphylococcus aureus* and *Pseudomonas aeruginosa*. The increase in concentration of Ag-Pd BNPs from 20 µg/mL to 200 µg/mL showed a notable enhancement in the cytotoxic anticancer activity against the human lung cancer cell line (A549). Therefore, the antimicrobial properties of the Ag-Pd BNPs (~20 nm) derived from the non-toxic fruit extract of *Terminalia chebula* suggest that Ag-Pd BNPs (~21 nm) synthesized using the eco-friendly and non-toxic leaf extract of *Citrus limon* may also possess potential antimicrobial activity, attributed to their < 25 nm size. The catalytic potential of Ag-Pd BNPs appears promising and is subject to variation based on the differential composition in the Ag to Pd ratios. For instance, Lu et al. (2014) [29] reported the synthesis of Ag-Pd BNPs using *Cacumen platycladi* leaf extract in varying ratios of Ag:Pd, exhibited sizes of 11.9 ± 0.8 nm (3:1), 9.1 ± 0.7 nm (1:1), and 7.4 ± 0.4 nm (1:3) and demonstrated that Ag-Pd BNPs in a 1:3 ratio, supported by γ-Al2O3 catalyst, were particularly effective in the hydrogenation of 1,3-butadiene compared to the other two ratios of Ag:Pd. This study not only reveals the influence of different ratios on the mean particle size but also highlights the variations in catalytic efficiency among the formed formulations. A study on mono-and bimetallic NPs of Ag and Pd was analyzed by Turunc et al. (2017) [30], they synthesized monometallic Ag NPs and Pd NPs, and bimetallic Ag-Pd BNPs using *Lithodora hispidula* leaf extract. These nanoparticles were employed to modify glassy carbon electrodes (GCE), resulting in the production of Ag NPs-GCE, Pd NPs-GCE, and Ag-Pd

BNPs-GCE for the electrocatalytic reduction of hydrogen peroxide (H_2O_2). Among these, Ag-Pd BNPs-GCE demonstrated superior efficiency, attributed to its increased synergistic catalytic effect, and exhibited a low detection limit, making it a more promising material to produce an H_2O_2 nanosensor. The enhanced efficiency of Ag-Pd BNPs over Ag NPs and Pd NPs alone underscores the importance of bimetallic-based experimental studies to achieve optimum catalytic efficiency based on metal combinations. On the other hand, Singh et al. (2020) [34] demonstrated the synthesis of nanoparticles using a single biomolecule, rutin. This study also involved the synthesis of both monometallic Ag NPs (~ 50 nm), Pd NPs (~ 10 nm), and bimetallic Ag-Pd (1:1) BNPs (~ 80 nm). These nanoparticles exhibited distinct catalytic activities in etherification reactions with phenolic compounds, with the order of reactivity being Pd NPs > Ag NPs > Ag-Pd BNPs. Notably, the smaller particle size (Pd NPs) displayed the highest reactivity among the three types. This highlights the importance of size-specific catalytic activity of the nanoparticles. Achieving a lower size of Ag-Pd BNPs, as done by the extract of fruit extract of *Terminalia chebula* [33], gum kondagogu extract [31] and in the current study through leaf extract of *Citrus limon* mediated Ag-Pd BNPs, could enhance efficiency. Therefore, testing whether this enhanced activity is due to the properties of the metal or the size of the overall nanoparticles is also required. Mohan et al. (2021) [28] utilized *Catharanthus roseus* mediated Ag-Pd BNPs (15–30 nm), which exhibited a remarkable 98% photocatalytic degradation of safranin O textile dye within 40 min of exposure. Moreover, they demonstrated a free radical scavenging efficiency of 70.2% (Ag-Pd BNPs), surpassing the 48.2% achieved by the leaf extract. Here, the enhanced efficiency can be attributed to the smaller size and unique properties of the synthesized Ag-Pd BNPs. Other combinations involving Au salts were compared by Velpula et al. (2021) [31], who demonstrated the synthesis of Ag-Au BNPs, Ag-Pd BNPs, and Au–Pd BNPs mediated by the gum kondagogu extract of the plant *Cochlospermum gossypium*. These nanoparticles were tested for their efficiency in catalyzing the reduction of 4-nitrophenol (4-NP). The results revealed catalytic efficiencies in the order of Ag-Pd BNPs (5–40 nm) > Ag-Au BNPs (2–40 nm) > Au–Pd BNPs (4–35 nm). This suggests that, for certain reactions, the properties dependent on the elemental composition are as significant as the size-related activity of the synthesized nanoparticles.

In contrast to our current findings on *Citrus limon*-mediated Ag-Pd BNPs, our previous studies on *Citrus limon*-mediated Au–Pd BNPs (Minal and Prakash (2020) [27]) exhibited unique characteristics and distinct bioassay results. UV–VIS spectroscopy analysis for Au–Pd BNPs revealed the presence of an SPR band around 540 nm due to the Au content, while the SPR band related to Ag was absent in the current Ag-Pd BNPs studies. The mean particle size of *Citrus limon*-mediated Au–Pd BNPs was 9.3 nm ± 3.95 nm, whereas our current studies observed a larger particle size of 21 nm ± 7.22 nm for Ag-Pd BNPs. DLS analysis indicated a size range of 150–200 nm with a Z-average of 3340 nm for Au–Pd BNPs, compared to the present DLS analysis with a Z-average of 1956 nm and the hydrodynamic size range of 800–1050 nm for Ag-Pd BNPs. Despite utilizing the same reducing agent, the observed variation in particle size was evident. Furthermore, the efficacy of *Citrus limon*-mediated Au–Pd BNPs nanotoxicity bioassay against I, II, III, and IV instar larvae of *Anopheles stephensi* and *Aedes aegypti* showed higher LC_{50} values compared to the lower LC_{50} values observed in the present study of Ag-Pd BNPs nanotoxicity bioassay. The LC_{50} values against I – IV instar larvae of *Anopheles stephensi* in the previously reported Au–Pd BNPs test were 5.12 mL/L, 8.14 mL/L, 26.32 mL/L, and 11.4 mL/L at 24 h, respectively, while LC_{50} values of 0.1 mL/L, 1.59 mL/L, 1.78 mL/L, and 1.62 mL/L at 24 h, respectively, were observed for the current Ag-Pd BNPs test. Similarly, for the previously reported Au–Pd BNPs, LC_{50} values of 12.37 mL/L, 11.24 mL/L, 6.17 mL/L, and 10.83 mL/L at 24 h against *Aedes aegypti* were reported, compared to current Ag-Pd BNPs test with observed LC_{50} values of 0.1 mL/L, 1.59 mL/L, 1.78 mL/L, and 2.08 mL/L at 24 h, respectively. The predation efficiency of non-target nymphs of dragonfly and damselfly under the Au–Pd BNPs test (6.67 mL/L) showed complete predation at 40 h for *Anopheles stephensi* with dragonfly nymph, while for other tests, including *Anopheles stephensi* with damselfly nymph, *Aedes aegypti* with dragonfly nymph, and *Aedes aegypti* with damselfly nymph, complete predation occurred at 48 h. In contrast, the current predation efficiency results under the Ag-Pd BNPs test (1.78 mL/L) showed 100% predation for *Aedes aegypti* with damselfly nymph at 24 h, and for other tests, 100% predation was achieved at 40 h. Therefore, understanding the characteristic and toxic differences between Au–Pd BNPs and Ag-Pd BNPs synthesized using the same reducing agent is crucial for determining their suitability in specific applications. This is especially important given that Au-containing BNPs demonstrate toxicity at higher concentrations, in contrast to Ag-containing BNPs, which exhibit toxicity at lower concentrations.

A pre-requisite to address the potential environmental implications of the synthesized nanoparticles, it is crucial to acknowledge that products incorporating metal nanoparticles, such as silver, titanium, zinc, gold, magnesium, aluminum oxide, copper, platinum, iron, and iron oxides, are

readily accessible in the consumer market. Moreover, the incorporation of these materials into new products is on a continuous rise [84]. The increasing industrial and household applications raise the likelihood of nanoparticles being released into the environment. Consequently, assessing the risk of nanoparticles-mediated ecotoxicity is crucial to formulate specific guidelines for their use, disposal, and bioremediation, and implementing strict surveillance for their accidental or intentional environmental release. Despite the numerous benefits, unknown risks may be associated with direct and indirect exposure to nanoparticles. The environmental impact and economic costs associated with the environmental release of nanoparticles are still underdeveloped. The majority of nanoparticle-based products are under study, awaiting industrial-level production, while others are already available in the market [85–87]. These nanoparticle-based products largely end up in soil, air, and aquatic environments. The nanoparticles contaminate soil, adversely affecting its enzymatic activity, nutritional balance, and self-cleaning properties. This, in turn, has a negative impact on beneficial microbial biodiversity, leading to adverse effects on plant growth and development, as well as bioaccumulation in both edible and non-edible plant tissues. Additionally, the leaching of nanoparticles into nearby aquatic reservoirs further impacts other ecological organisms [88]. Whereas, the optimal use of some metal nanoparticles such as iron and gold in clinical trial studies, specifically for theragnostic and radiotherapy applications, is closely observed, and the final formulation is approved or rejected based on associated implications on human health [89]. However, the unintentional environmental release of nanoparticles from nano-biocomposites used in food packaging technologies is not as closely monitored. This calls for the establishment of standard guidelines to test the ecotoxicological effects of nanoparticles released from packaging materials [90]. The field of environmental nanotechnology actively engages in providing solutions to address the environmental impact, cleanup, and remediation of anthropogenic nanomaterials. Many of these solutions involve the use of mono- and bi-metallic nanoparticles to remove other nano-contaminants, which still pose the risk of contaminating the environment themselves due to high mobility and transport, leading to unintended contamination, creation of toxic byproducts during remediation, and toxicity to local flora and fauna. The short-term stability and persistence of these nanoparticles further pose risks to the environment, leading to bioaccumulation and biomagnification. Additionally, unknown interactions in the environment can lead to the generation of new and harmful compounds. Consequently, bimetallic nanoparticles are observed to play a dual role depending on the mode of application, serving either as a contaminant or as an agent for the remediation of other nano-contaminants [91]. The environmental implications of adverse effects of nanoparticles are high due to their large surface area to volume ratio. Ongoing research on nanoparticles transport, environmental fate, long-term effects, and potential risks associated with their use in remediation, based on the specific characteristics of the nanoparticles, is evident in recent literature. Furthermore, regulatory frameworks are being developed by the U.S., European Union, Canada, Australia, and International Collaborations. These frameworks, such as the Toxic Substances Control Act (TSCA) under the U.S. Environmental Protection Agency (EPA), the Registration, Evaluation, Authorization, and Restriction of Chemicals (REACH) regulation, Canadian Environmental Protection Act (CEPA), National Industrial Chemicals Notification and Assessment Scheme (NICNAS), and Organization for Economic Co-operation and Development (OECD), respectively, are formulating guidelines for the responsible use of nanotechnology in environmental applications. This involves collaboration between governments, industry stakeholders, and scientific communities to ensure that regulations are supported by the latest scientific understanding and technological advancements [92–94].

Lastly, the limitation of the biologically synthesized nanoparticles lies in the use of diverse leaf extracts, each containing a unique phytochemical composition, which play a distinctive role in the synthesis of nanoparticles, resulting in variations in the size and shape that subsequently influence their toxicity and other properties. A significant limitation in the available literature lies in the lack of comprehensive comparisons concerning the toxicities observed in bioassays of biologically synthesized nanoparticles. This limitation arises due to the frequent use of units like ppm without disclosing the actual amount of the formulation used for experiments. The common reliance on ppm as a measurement unit, often employed by researchers, fails to provide a clear understanding of the nanoparticles' original specifications employed in the tests. Given the inherent variability in the size and shape of biologically synthesized nanoparticles, the use of ppm becomes less than ideal. A more suitable approach can involve comparing size-related characterizations (SEM, TEM, DLS) with toxicity results presented as raw measurements in units of mL/ng/mg/% of NPs in solvent (units). Additionally, specifying the applied serial dilution of the molar solution during experimentation is imperative.

The current study provides significant information about the novel characteristic features of Ag-Pd BNPs synthesized using a non-toxic *Citrus limon* leaf extract for the first time. It also addresses a critical gap by conducting the first-ever nanotoxicity evaluation of Ag-Pd BNPs against more complex environmental invertebrates. Therefore, moving ahead toward ecotoxicological

evaluation compared to the available studies on simpler laboratory based antimicrobial and anticancer assays. In addition to the mosquito larvicidal efficacy of Ag-Pd BNPs, studies against non-target nymphs are required for the selection of the minimal effective concentration. This would help to formulate a sustainable, target-oriented insecticide posing a comparatively lower threat to non-target organisms. Therefore, we recommend that for pest management, simultaneous efficacies against non-target organisms spatially present in the same niche as the target pest should be considered complementary in selecting nanoparticles concentrations. The LC_{50} value varies among environmental organisms and life stages, influenced by their biological complexities. Our findings are consistent with other existing literature, highlighting the potential applicability of *Citrus limon* mediated Ag-Pd BNPs in catalytic, antimicrobial, and anticancer activities.

Conclusion

This study highlights the eco-friendly synthesis of Ag-Pd BNPs using a biodegradable, nontoxic aqueous leaf extract of plant *Citrus limon.* Characterization confirmed successful synthesis with physicochemical properties suitable for antimicrobial and catalytic applications. The synthesized Ag-Pd BNPs demonstrated larvicidal efficacy against all larval stages of *Anopheles stephensi* and *Aedes aegypti* mosquitoes, while showing no toxicity to selected non-target organisms, indicating dose-dependent effects. Future studies should focus on optimizing concentrations tailored to specific applications, such as nanosensors, nanocatalysts, and antimicrobial formulations. However, the potential eco-toxicity of Ag-Pd BNPs due to environmental leakage underscores the need for comprehensive toxicity assessments and strict regulatory measures to prevent harm to sensitive species. With proper safety and bioremediation strategies, Ag-Pd BNPs could be sustainably utilized against resistant microbial strains and insecticide-resistant vectors. Eco-friendly bio-insecticidal formulations with minimal effective concentrations warrant further exploration for environmentally conscious applications.

Supplementary Information

The online version contains supplementary material available at https://doi.org/10.1186/s44331-025-00001-7.

Supplementary Material 1.

Acknowledgements
We sincerely acknowledge our gratitude towards Prof. P. S. Satsangi (Chairman, Advisory Committee on Education), and Prof. P.K. Kalra (Director), Dayalbagh Educational Institute (DEI), Agra. We thank Head, Department of Zoology, DEI, for materials and instruments. We thank Head, Department of Chemistry for, XRD, FTIR spectroscopy facility (for leaf extract), and Zetasizer facility, at the instrumentation lab, DEI. We thank Prof. Tapas Chandra Nag for TEM facility (SAIF, AIIMS, Delhi), Prof. Dinesh Mohan for SEM-EDX spectroscopy facility, AIRF, (JNU, Delhi), and Prof. S. A. Ansari for FTIR and UV-Vis spectroscopy facility (for Ag-Pd BNPs), CIF (Jamia Millia Islamia, Delhi).

Authors' contributions
S.P.M. has contributed to the methodology, experimentation, analysis, drafting, and reviewing of the original manuscript. S.P. has conceptualized the research, provided supervision throughout the study, and contributed to the reviewing of the manuscript.

Funding
Not applicable.

Data availability
No datasets were generated or analysed during the current study.

Declarations

Ethics approval and consent to participate
Not applicable.

Competing interests
Authors may have a conflict of interest with a New Delhi (Capital City of India) based reviewer who might reject the article due to personal reasons. Therefore, we request to not send to any New Delhi/Delhi, India-based reviewer.

Received: 6 October 2024 Accepted: 3 January 2025
Published online: 07 February 2025

References

1. Das RK, Pachapur VL, Lonappan L, Naghdi M, Pulicharla R, Maiti S, et al. Biological synthesis of metallic nanoparticles: plants, animals and microbial aspects. Nanotechnol Environ Eng. 2017;2:1–21.
2. Berta L, Coman NA, Rusu A, Tanase C. A review on plant-mediated synthesis of bimetallic nanoparticles, characterisation and their biological applications. Materials. 2021;14(24):7677.
3. FeiGuo C, Sun T, Cao F, Liu Q, Ren Z. Metallic nanostructures for light trapping in energy-harvesting devices. Light. 2014;3(4):e161–e161.
4. A. Elangovan M, Santhoshkumar M, Selvaraj K, Sathishkumar K, Kumar M, Jothinathan MKD, et al. Sunlight-driven photocatalytic and anticancer properties of biogenic synthesized gold nanoparticles (AuNPs) employing Polygala elongata. J King Saud Univ Sci. 2024;36(5):103158.
5. Moslah C, Kandyla M, Mousdis GA, Petropoulou G, Ksibi M. Photocatalytic properties of titanium dioxide thin films doped with noble metals (Ag, Au, Pd, and Pt). Phys Status Solidi (a). 2018;215(17):1800023.
6. Narenkumar J, Parthipan P, Madhavan J, Murugan K, Marpu SB, Suresh AK, Rajasekar A. Bioengineered silver nanoparticles as potent anticorrosive inhibitor for mild steel in cooling towers. Environ Sci Pollut Res. 2018;25:5412–20.
7. El-Shamy OA, Deyab MA. Eco-friendly biosynthesis of silver nanoparticles and their improvement of anti-corrosion performance in epoxy coatings. J Mol Liq. 2023;376:121488.
8. Zhang J, Ahmadi M, Fargas G, Perinka N, Reguera J, Lanceros-Méndez S, et al. Silver nanoparticles for conductive inks: from synthesis and ink formulation to their use in printing technologies. Metals. 2022;12(2):234.
9. Mandal D, Mishra S, Singh RK. Green synthesized nanoparticles as potential nanosensors. Environ Chem Med Sensors. 2018;137:164.
10. Jebril S, Fdhila A, Dridi C. Nanoengineering of eco-friendly silver nanoparticles using five different plant extracts and development of cost-effective phenol nanosensor. Sci Rep. 2021;11(1):22060.
11. Rana A, Yadav K, Jagadevan S. A comprehensive review on green synthesis of nature-inspired metal nanoparticles: mechanism, application and toxicity. J Clean Prod. 2020;272:122880.

12. Mukherjee S, Patra CR. Biologically synthesized metal nanoparticles: recent advancement and future perspectives in cancer theranostics. Future Sci OA. 2017;3(3):FSO203.
13. Kuchur OA, Tsymbal SA, Shestovskaya MV, Serov NS, Dukhinova MS, Shtil AA. Metal-derived nanoparticles in tumor theranostics: Potential and limitations. J Inorg Biochem. 2020;209:111117.
14. HabeebRahuman HB, Dhandapani R, Narayanan S, Palanivel V, Paramasivam R, Subbarayalu R, et al. Medicinal plants mediated the green synthesis of silver nanoparticles and their biomedical applications. IET Nanobiotechnol. 2022;16(4):115–44.
15. Manimaran K, Yanto DHY, Anita SH, Nurhayat OD, Selvaraj K, Basavarajappa S, et al. Synthesis and characterization of Hypsizygus ulmarius extract mediated silver nanoparticles (AgNPs) and test their potentiality on antimicrobial and anticancer effects. Environ Res. 2023;235:116671.
16. Faisal S, Ullah R, Alotaibi A, Zafar S, Rizwan M, Tariq MH. Biofabrication of silver nanoparticles employing biomolecules of Paraclostridium benzoelyticum strain: Its characterization and their in-vitro antibacterial, anti-aging, anti-cancer and other biomedical applications. Microscopy Research and Technique. 2023.
17. Faisal S, Khan MA, Jan H, Shah SA, Shah S, Rizwan M, Akbar MT. Edible mushroom (Flammulina velutipes) as biosource for silver nanoparticles: from synthesis to diverse biomedical and environmental applications. Nanotechnology. 2020;32(6):065101.
18. Al-Radadi NS, Hussain T, Faisal S, Shah SAR. Novel biosynthesis, characterization and bio-catalytic potential of green algae (Spirogyra hyalina) mediated silver nanomaterials. Saudi J Biolog Sci. 2022;29(1):411–9.
19. Soni N, Prakash S. Silver nanoparticles: a possibility for malarial and filarial vector control technology. Parasitol Res. 2014;113:4015–22.
20. Verma A, Preet S. Novel green synthesis of combinational silver nanoparticles using jatropha integerrima for dengue vector control and cytotoxicity Assessment. Proc National Acad Sci India Section B Biolog Sci. 2022;92(4):747–57.
21. Almatroudi A. Unlocking the potential of silver nanoparticles: from synthesis to versatile bio-applications. Pharmaceutics. 2024;16(9):1232.
22. Osman AI, Zhang Y, Farghali M, Rashwan AK, Eltaweil AS, Abd El-Monaem EM, et al. Synthesis of green nanoparticles for energy, biomedical, environmental, agricultural, and food applications: a review. Environ Chemist Lett. 2024;22(2):841–87.
23. Ahmed B, Tahir MB, Sagir M, Hassan M. Bio-inspired sustainable synthesis of silver nanoparticles as next generation of nanoproduct in antimicrobial and catalytic applications. Mater Sci Eng, B. 2024;301:117165.
24. Vishnukumar P, Vivekanandhan S, Muthuramkumar S. Plant-mediated biogenic synthesis of palladium nanoparticles: recent trends and emerging opportunities. ChemBioEng Reviews. 2017;4(1):18–36.
25. Kim K, Kim KL, Shin KS. Co-reduced Ag/Pd bimetallic nanoparticles: surface enrichment of Pd revealed by Raman spectroscopy. J Phys Chemist C. 2011;115(30):14844–51.
26. Wong ST, Shamsuddin M, Alizadeh A, Yun YS. In-situ generated palladium seeds lead to single-step bioinspired growth of AuPd bimetallic nanoparticles with catalytic performance. Mater Chem Phys. 2016;183:356–65.
27. Minal SP, Prakash S. Laboratory analysis of Au–Pd bimetallic nanoparticles synthesized with Citrus limon leaf extract and its efficacy on mosquito larvae and non-target organisms. Sci Rep. 2020;10(1):21610.
28. Mohan S, Devan MV, Sambathkumar S, Shanmugam V, Ravikumar K, Marnadu R, et al. Dual probes of Ag/Pd bimetallic NPs facilely synthesized by green process using Catharanthus leaf extract on textile dye removal and free radical capability. Appl Nanosci. 2021;11:1565–74.
29. Lu F, Sun D, Huang J, Du M, Yang F, Chen H, et al. Plant-mediated synthesis of Ag–Pd alloy nanoparticles and their application as catalyst toward selective hydrogenation. ACS Sustainable Chemist Eng. 2014;2(5):1212–8.
30. Turunc E, Binzet R, Gumus I, Binzet G, Arslan H. Green synthesis of silver and palladium nanoparticles using Lithodora hispidula (Sm.) Griseb. (Boraginaceae) and application to the electrocatalytic reduction of hydrogen peroxide. Mater Chem Phys. 2017;202:310–9.
31. Velpula S, Beedu SR, Rupula K. Bimetallic nanocomposite (Ag-Au, Ag-Pd, Au-Pd) synthesis using gum kondagogu a natural biopolymer and their catalytic potentials in the degradation of 4-nitrophenol. Int J Biol Macromol. 2021;190:159–69.
32. Abdel-Fattah WI, Eid MM, Abd El-Moez SI, Mohamed E, Ali GW. Synthesis of biogenic Ag@ Pd Core-shell nanoparticles having anticancer/antimicrobial functions. Life Sci. 2017;183:28–36.
33. Sivamaruthi BS, Ramkumar VS, Archunan G, Chaiyasut C, Suganthy N. Biogenic synthesis of silver palladium bimetallic nanoparticles from fruit extract of Terminalia chebula–In vitro evaluation of anticancer and antimicrobial activity. J Drug Deliv Sci Technol. 2019;51:139–51.
34. Singh P, Halder M, Ray S, Bose A, Sen K. Green synthesis of silver and palladium nanocomposites: a study of catalytic activity towards etherification reaction. Materials Adv. 2020;1(8):2937–52.
35. Li C, Han Y, Gao T, Zhang J, Xu DX, Wâng Y. Insecticidal activity of metallic nanopesticides synthesized from natural resources: a review. Environ Chem Lett. 2023;21(2):1141–76.
36. Onen H, Luzala MM, Kigozi S, Sikumbili RM, Muanga CJK, Zola EN, et al. Mosquito-borne diseases and their control strategies: an overview focused on green synthesized plant-based metallic nanoparticles. Insects. 2023;14(3):221.
37. Pouthika K, Madhumitha G. A review on plant-derived nanomaterials: an effective and innovative insect-resistant strategy for alternate pesticide development. Int J Environ Sci Technol. 2023;21:1–24.
38. Nie D, Li J, Xie Q, Ai L, Zhu C, Wu Y, et al. Nanoparticles: a potential and effective method to control insect-borne diseases. Bioinorg Chemist Appl. 2023;2023:5898160.
39. Minal, S. P., & Prakash, S. Cu–Zn and Ag–Cu bimetallic nanoparticles as larvicide to control malaria parasite vector: a comparative analysis. In 2016 IEEE region 10 Humanitarian technology conference (R10-HTC) (1–6) (IEEE, 2016).
40. Minal SP, Prakash S. Characterization and nano-efficacy study of palladium nanoparticles against Larvae of Anopheles stephensi (Liston). Int J Adv Eng Nanotechnol. 2018;3(10):1–5.
41. Minal PS, Prakash S. Efficacy of bimetallic copper-zinc nanoparticles against larvae of microfilariae vector in laboratory. Int J Sci Res. 2019;8(2):1–4.
42. World malaria report 2023 https://www.who.int/teams/global-malaria-programme/reports/world-malaria-report-2023.
43. Tolle MA. Mosquito-borne diseases. Curr Probl Pediatr Adolesc Health Care. 2009;39(4):97–140.
44. Vector-borne diseases - World Health Organization (WHO) (https://www.who.int/news-room/fact-sheets/detail/vector-borne-diseases).
45. Brugueras S, Fernández-Martínez B, Martínez-de la Puente J, Figuerola J, Porro TM, Rius C, et al. Environmental drivers, climate change and emergent diseases transmitted by mosquitoes and their vectors in southern Europe: a systematic review. Environ Res. 2020;191:110038.
46. Filho WL, Scheday S, Boenecke J, Gogoi A, Maharaj A, Korovou S. Climate change, health and mosquito-borne diseases: trends and implications to the pacific region. Int J Environ Res Public Health. 2019;16(24):5114.
47. Franklinos LH, Jones KE, Redding DW, Abubakar I. The effect of global change on mosquito-borne disease. Lancet Infect Dis. 2019;19(9):e302–12.
48. Rani A, Gupta A, Nagpal BN, Gupta SK, Prasad P, Singh H. Impact of urbanization on the abundance and distribution of anophelines population in Ghaziabad district, Uttar Pradesh India. J Vector Borne Dis. 2023;61(1):29–42.
49. World Health Organization, & UNICEF. (2017). Global vector control response 2017–2030.
50. Govindarajan M, Rajeswary M, Muthukumaran U, Hoti SL, Khater HF, Benelli G. Single-step biosynthesis and characterization of silver nanoparticles using Zornia diphylla leaves: a potent eco-friendly tool against malaria and arbovirus vectors. J Photochem Photobiol, B. 2016;161:482–9.
51. Govindarajan M, Khater HF, Panneerselvam C, Benelli G. One-pot fabrication of silver nanocrystals using Nicandra physalodes: a novel route for mosquito vector control with moderate toxicity on non-target water bugs. Res Vet Sci. 2016;107:95–101.
52. Foko LPK, Meva FEA, Moukoko CEE, Ntoumba AA, Ekoko WE, Belle PEK, et al. Green-synthesized metal nanoparticles for mosquito control: a systematic review about their toxicity on non-target organisms. Acta Tropica. 2021;214:105792.
53. Salayová A, Bedlovičová Z, Daneu N, Baláž M, Lukáčová Bujňáková Z, Balážová Ľ, Tkáčiková Ľ. Green synthesis of silver nanoparticles with antibacterial activity using various medicinal plant extracts: Morphology and antibacterial efficacy. Nanomaterials. 2021;11(4):1005.
54. Borase HP, Salunke BK, Salunkhe RB, Patil CD, Hallsworth JE, Kim BS, Patil SV. Plant extract: a promising biomatrix for ecofriendly, controlled synthesis of silver nanoparticles. Appl Biochem Biotechnol. 2014;173:1–29.

55. Rajan DS, Varghese TA. An evaluation on the larvicidal efficacies of aqueous leaf extracts of Lantana camara and Catharanthus roseus against mosquito larvae. Int J Mosquito Res. 2017;4(3):93–7.
56. Zahr S, Zahr R, El Hajj R, Khalil M. Phytochemistry and biological activities of Citrus sinensis and Citrus limon: An update. J Herbal Med. 2023;15:100737.
57. WRBU: Mosquito Identification Resources http://www.wrbu.org/VecID_MQ.htmL.
58. World Health Organization. Guidelines for laboratory and field testing of mosquito larvicides (No. WHO/CDS/WHOPES/GCDPP/2005.13). World Health Organization. 2005.
59. Odonata | Species | India Biodiversity Portal Bradinopyga geminata (Rambur, 1842). https://indiabiodiversity.org/species/show/226725?pos=.
60. Odonata | Species | India Biodiversity Portal Ischnura senegalensis (Rambur, 1842).https://indiabiodiversity.org/species/show/234358?pos=.
61. Saha N, Aditya G, Banerjee S, Saha GK. Predation potential of odonates on mosquito larvae: implications for biological control. Biol Control. 2012;63(1):1–8.
62. Murugan K, Nataraj D, Madhiyazhagan P, Sujitha V, Chandramohan B, Panneerselvam C, et al. Carbon and silver nanoparticles in the fight against the filariasis vector Culex quinquefasciatus: genotoxicity and impact on behavioral traits of non-target aquatic organisms. Parasitol Res. 2016;115:1071–83.
63. Ferreira T, Rasband W. ImageJ user guide. ImageJ/Fiji. 2012;1:155–61.
64. Abbott WS. A method of computing the effectiveness of insecticides. J Ecol Entomol. 1925;18:265–7.
65. Finney DJ, Stevens WL. A table for the calculation of working probits and weights in probit analysis. Biometrika. 1948;35(1–2):191–201.
66. Finney DJ, editor. Probit Analysis. Cambridge: Cambridge University Press; 1952.
67. Coates J. Interpretation of infrared spectra, a practical approach. Encyclop Analyt Chemist. 2000;12:10815–37.
68. Origin(Pro), 2023. OriginLab Corporation, Northampton, MA, USA.
69. Yeap SP, Lim J, Ngang HP, Ooi BS, Ahmad AL. Role of particle–particle interaction towards effective interpretation of Z-average and particle size distributions from dynamic light scattering (DLS) analysis. J Nanosci Nanotechnol. 2018;18(10):6957–64.
70. Souza TG, Ciminelli VS, Mohallem NDS. A comparison of TEM and DLS methods to characterize size distribution of ceramic nanoparticles. J Phys Confer Ser. 2016;733(1):012039 IOP Publishing.
71. Bhattacharjee S. DLS and zeta potential–what they are and what they are not? J Control Release. 2016;235:337–51.
72. Soni N, Prakash S. Entomopathogenic fungus generated Nanoparticles for enhancement of efficacy in Culex quinquefasciatus and Anopheles stephensi. Asian Pacific J Trop Dis. 2012;2:S356–61.
73. Bhakyaraj K, Kumaraguru S, Gopinath K, Sabitha V, Kaleeswarran PR, Karthika V, et al. Eco-friendly synthesis of palladium nanoparticles using Melia azedarach leaf extract and their evaluation for antimicrobial and larvicidal activities. J Cluster Sci. 2017;28:463–76.
74. Kalimuthu K, Panneerselvam C, Chou C, Tseng LC, Murugan K, Tsai KH, et al. Control of dengue and Zika virus vector Aedes aegypti using the predatory copepod Megacyclops formosanus: synergy with Hedychium coronarium-synthesized silver nanoparticles and related histological changes in targeted mosquitoes. Process Safety Environ Protect. 2017;109:82–96.
75. Fouad H, Hongjie L, Hosni D, Wei J, Abbas G, Ga'al H, Jianchu M. Controlling Aedes albopictus and Culex pipiens pallens using silver nanoparticles synthesized from aqueous extract of Cassia fistula fruit pulp and its mode of action. Artificial Cells Nanomed Biotechnol. 2018;46(3):558–67.
76. Ga'al H, Fouad H, Tian J, Hu Y, Abbas G, Mo J. Synthesis, characterization and efficacy of silver nanoparticles against Aedes albopictus larvae and pupae. Pestic Biochem Physiol. 2018;144:49–56.
77. dos Santos Lima JC, Moreira RA, Neto AJG, de Pádua Andrade D, Freitas EC, Daam MA, Rocha O. Metal Toxicity can affect dragonfly nymphs and ostracods predation rates and food selectivity: ecological implications on food webs. Water Air Soil Pollut. 2021;232:1–12.
78. Azam I, Afsheen S, Zia A, Javed M, Saeed R, Sarwar MK, Munir B. Evaluating insects as bioindicators of heavy metal contamination and accumulation near industrial area of Gujrat, Pakistan. BioMed research international. 2015;2015:942751.
79. Akhtar ZR, Tariq K, Mavian C, Ali A, Ullah F, Zang LS, et al. Trophic transfer and toxicity of heavy metals from dengue mosquito Aedes aegypti to predator dragonfly Tramea cophysa. Ecotoxicology. 2021;30(6):1108–15.
80. Murugan K, Dinesh D, Kumar PJ, Panneerselvam C, Subramaniam J, Madhiyazhagan P, et al. Datura metel-synthesized silver nanoparticles magnify predation of dragonfly nymphs against the malaria vector Anopheles stephensi. Parasitol Res. 2015;114:4645–54.
81. Murugan K, Benelli G, Ayyappan S, Dinesh D, Panneerselvam C, Nicoletti M, et al. Toxicity of seaweed-synthesized silver nanoparticles against the filariasis vector Culex quinquefasciatus and its impact on predation efficiency of the cyclopoid crustacean Mesocyclops longisetus. Parasitol Res. 2015;114:2243–53.
82. Murugan K, Panneerselvam C, Subramaniam J, Madhiyazhagan P, Hwang JS, Wang L, et al. Eco-friendly drugs from the marine environment: spongeweed-synthesized silver nanoparticles are highly effective on Plasmodium falciparum and its vector Anopheles stephensi, with little non-target effects on predatory copepods. Environ Sci Poll Res. 2016;23:16671–85.
83. Kalimuthu K, Panneerselvam C, Chou C, Lin SM, Tseng LC, Tsai KH, et al. Predatory efficiency of the copepod Megacyclops formosanus and toxic effect of the red alga Gracilaria firma-synthesized silver nanoparticles against the dengue vector Aedes aegypti. Hydrobiologia. 2017;785:359–72.
84. Vance ME, Kuiken T, Vejerano EP, McGinnis SP, Hochella MF Jr, Rejeski D, Hull MS. Nanotechnology in the real world: Redeveloping the nanomaterial consumer products inventory. Beilstein J Nanotechnol. 2015;6(1):1769–80.
85. Stark W, et al. Industrial applications of nanoparticles. Chem Soc Rev. 2015;44(16):5793–805.
86. Nowack B, Bucheli TD. Occurrence, behavior and effects of nanoparticles in the environment. Environ Pollut. 2007;150(1):5–22.
87. Taghavi SM, Momenpour M, Azarian M, Ahmadian M, Souri F, Taghavi SA, et al. Effects of nanoparticles on the environment and outdoor workplaces. Electronic Phys. 2013;5(4):706.
88. Rajput VD, Minkina T, Sushkova S, Tsitsuashvili V, Mandzhieva S, Gorovtsov A, et al. Effect of nanoparticles on crops and soil microbial communities. J Soils Sediments. 2018;18:2179–87.
89. Bobo D, Robinson KJ, Islam J, Thurecht KJ, Corrie SR. Nanoparticle-based medicines: a review of FDA-approved materials and clinical trials to date. Pharm Res. 2016;33:2373–87.
90. Adeyemi JO, Fawole OA. Metal-based nanoparticles in food packaging and coating technologies: a review. Biomolecules. 2023;13(7):1092.
91. Patil SS, Shedbalkar UU, Truskewycz A, Chopade BA, Ball AS. Nanoparticles for environmental clean-up: a review of potential risks and emerging solutions. Environ Technol Innov. 2016;5:10–21.
92. Ali F, Neha K, Parveen S. Current regulatory landscape of nanomaterials and nanomedicines: A global perspective. J Drug Deliv Sci Technol. 2022;80:104118.
93. Allan J, Belz S, Hoeveler A, Hugas M, Okuda H, Patri A, et al. Regulatory landscape of nanotechnology and nanoplastics from a global perspective. Regul Toxicol Pharmacol. 2021;122:104885.
94. Mohammadi Z, Jafari SM. Regulatory principles on food nanoparticles legislated by Asian and Oceanian countries. In *Safety and Regulatory Issues of Nanoencapsulated Food Ingredients*. 2021.(pp. 201–238). Academic Press.

Publisher's Note